Hidden biosphere in an oxygen-deficient Atlantic open ocean eddy: Future implications of ocean deoxygenation on primary production in the eastern tropical North Atlantic

C. R. Löscher[1]*, M. A. Fischer[1†], S. C. Neulinger[1†], B. Fiedler[2], M. Philippi[1], F. Schütte[2], A. Singh[2#], H. Hauss[2], J. Karstensen[2], A. Körtzinger[2,3], S. Künzel[4], R. A. Schmitz[1]

[1] Institute for General Microbiology, Kiel, Germany

[2] GEOMAR, Helmholtz Centre for Ocean Research Kiel, Kiel University, Germany

Now at: Physical Research Laboratory, Geosciences Division, Ahmedabad, India 380 009

[3] Christian-Albrechts-Universität zu Kiel, Kiel, Germany

[4] Max Planck Institute for Evolutionary Biology, Plön, Germany

* Correspondence should be addressed to cloescher@geomar.de

† Equal contribution.

The eastern tropical North Atlantic (ETNA) is characterized by a highly productive coastal upwelling system and a moderate oxygen minimum zone with lowest open ocean oxygen (O_2) concentrations of approximately 40 µmol kg^{-1}. The recent discovery of re-occurring mesoscale eddies with close to anoxic O_2 concentrations (<1 µmol kg^{-1}) located just below the mixed layer has challenged our understanding of O_2 distribution and biogeochemical processes in this area.

Here, we present the first microbial community study from a deoxygenated anticyclonic modewater eddy in the open waters of the ETNA. In the eddy, we observed significantly lower bacterial diversity compared to surrounding waters, along with a significant community shift. We detected enhanced primary productivity in the surface layer of the eddy indicated by elevated chlorophyll concentrations and carbon uptake rates of up to three times as high as in surrounding waters. Carbon uptake rates below the euphotic zone correlated to the presence of a specific high-light ecotype of *Prochlorococcus*, which is usually underrepresented in the ETNA. Our data indicate that high primary production in the eddy fuels export production and supports enhanced respiration in a specific microbial community at shallow depths, below the mixed layer base. The O_2-depleted core waters eddy promoted transcription of the key gene for denitrification, *nirS*. This process is usually absent from the open ETNA waters.

In light of future projected ocean deoxygenation, our results show that even distinct events of anoxia have the potential to alter microbial community structure with critical impacts on primary productivity and biogeochemical processes of oceanic water bodies.

1 Introduction

The eastern tropical North Atlantic (ETNA) region is influenced by an eastern boundary upwelling system (EBUS) off northwest Africa, which along with nutrient supply via Saharan dust deposition, fuels one of the most productive ocean regions in the world. A moderate oxygen minimum zone (OMZ) is associated with this EBUS, with lowest oxygen (O_2) concentrations just below 40 μmol kg^{-1} present at intermediate depths (Chavez and Messié, 2009;Jickells et al., 2005;Karstensen et al., 2008).

O_2 records over several years from the Cape Verde Ocean Observatory (CVOO) mooring (located at 17° 35'N, 24° 15'W, Fig. 1) confirmed the well-ventilated character of the ETNA. However, the observation of distinct events of very low-O_2 concentrations (<1 μmol kg^{-1}) at depths around 40 to 100 m over periods of more than one month challenged our understanding of the biogeochemistry in that area (Karstensen et al., 2015a). The meridional current structure observed during these low-O_2 events revealed the passage of anticyclonic modewater eddies (ACME) crossing the CVOO mooring (Karstensen et al., 2015a). The ocean is filled with eddies (Chelton et al., 2011) but only a few of them have the dynamical and biogeochemical boundary conditions that support formation of a low-O_2 core. Anomalous low salinity within the ETNA low-O_2 eddies suggested the water mass originated from the EBUS off Mauritania, which was confirmed by analyzing sea-level anomaly data. In combination with other data from the upwelling region, Karstensen et al. (2015a) showed that O_2 concentrations decreased over a period of a few months during westward propagation of the eddies into the open north Atlantic Ocean. Respiration in these eddies was estimated to be about three to five times higher than typical subtropical gyre values (Karstensen et al., 2008).

Mesoscale eddies are increasingly recognized as biogeochemical hot-spots of basin-wide relevance for the world's oceans (Altabet et al., 2012;Baird et al., 2011;Chelton et al., 2011;McGillicuddy et al., 2007;Oschlies and Garcon, 1998;Stramma et al., 2013). Upward nutrient supply to the euphotic zone through mesoscale eddy dynamics enables intense primary productivity (Lévy et al., 2012;Lévy et al., 2001;McGillicuddy et al., 2007). Classically, primary producers in the ETNA open waters area are dominated by a range of diatom clades, flagellates and cyanobacteria (Franz et al., 2012), but so far no specific information on the primary producers in productive ETNA eddies has been reported. As a result of enhanced primary production in the surface, increased organic matter export flux below the euphotic zone is expected, which in turn supports increased respiration at intermediate depths. Indeed, particle maxima a few meters above the O_2 minimum have been reported based on autonomous observations of

O_2-depleted eddies in the ETNA (Karstensen et al., 2015a) indicating enhanced organic matter export and provide environments of enhanced remineralization (Ganesh et al., 2014). Observations from a low-O_2 eddy from the ETNA revealed a remarkable impact on all productivity-related processes in that particular system (Fischer et al., 2015). Estimated productivity was three-fold higher in the surface layer compared to surrounding waters along with a multiple times increase in mass flux in bathypelagic during the eddy passage. Furthermore, Fiedler et al. (in prep. for this special issue) determined export flux derived from carbon remineralization rates within the eddy and found a 3-4-fold enhanced export flux compared to background conditions in the open-ocean ETNA.

O_2-depleted conditions are supposed to act as a critical switch for the marine microbial community, both with regard to functionality and diversity. O_2 begins to limit oxidative pathways and reductive pathways are induced (Stewart et al., 2011;Ulloa et al., 2012;Wright et al., 2012). A loss in microbial diversity related to vertical O_2 gradients has previously been described for the Pacific Ocean (Beman and Carolan, 2013;Bryant et al., 2012), but to date no comparable data are available from the ETNA. O_2-loss related microbial community shifts and modified functionality are supposed to favor heterotrophic communities dominated by Flavobacteria, α- and γ- Proteobacteria, which efficiently recycle organic matter (Buchan et al., 2014). Furthermore, marine nitrogen (N) and carbon (C) cycling are significantly altered under low O_2 conditions (Vaquer-Sunyer and Duarte, 2008;Wright et al., 2012). Substantial N loss (Altabet et al., 2012) along with enhanced nitrous oxide production (Arévalo-Martínez et al., 2015) has been described in low-O_2 eddies in the OMZ off Peru in the eastern tropical South Pacific.
Classically, the N cycle in the open ETNA is assumed to be dominated by nitrification. An N loss signal is not present due to comparably high background O_2 concentrations (≥40 μmol kg^{-1},(Löscher et al., 2012;Ryabenko et al., 2012). However, any drop in O_2 concentration in the water column, as potentially induced by the low-O_2 eddies, could potentially activate anammox and/or denitrification. During recent decades, the ETNA OMZ has been expanding both in terms of vertical extent and intensity and is predicted to expand further in the future (Stramma et al., 2008) with unknown consequences for the ecology and biogeochemistry of that system. Thus, it is critical to understand the biogeochemical response to changing O_2 concentrations in that region.

In this study, we investigated differences in microbial community structure in an O_2-depleted eddy, surrounding ETNA open waters, and upwelled waters on the Mauritanian shelf. This was achieved using a combined high-throughput 16S rDNA amplicon sequencing/qPCR approach along with carbon uptake rate measurements and hydrochemical observations. This study aimed to understand the microbial community response to O_2 depleted conditions with regard to primary production and remineralization in these poorly-

described anomalies, to improve understanding of the sensitivity of the ETNA biogeochemistry to future ocean deoxygenation.

2 Material and Methods

2.1 Data collection

Remotely sensed sea level anomalies (SLA), in combination with temperature and salinity data measured by Argo floats (an overview is presented by Körtzinger et al., (2015) in preparation for this issue) were used for general eddy identification and tracking in this area. After identification of a low-O_2 eddy candidate that was propagating towards CVOO, a pre-survey was started using autonomous gliders (see Karstensen et al. (2015b), in preparation for this issue). Once the glider data had confirmed the low O_2 concentration in the candidate eddy, a ship-based survey was started. First, we performed a survey with the Cape Verdean RV Islandia on Mar 6, 2014 (samples from this survey are further referred to as eddy_1), followed by a second survey with the German RV Meteor (cruise M105; Mar 19, 2014; samples from this survey are further referred to as eddy_2). Moreover, the background signal (i.e. waters outside the eddy) was measured, in order to compare the eddy with the typical open ocean ETNA environment. For this purpose, we used metagenomic samples from the CVOO time series monitoring site (collected on 03/19/2014 during cruise M105). Samples from the Mauritanian shelf collected during R/VMeteor Cruise M107 (station 675, 18.22°N/ 16.56°W, collected on 06/24/2014) represent data from the eddy formation area. Station 675 was chosen according to its location within the area that Schütte et al. (2015, in preparation, this issue) identified as the region of eddy formation and further because of the observed low O_2 concentrations of 33.9 µmol kg^{-1} at 115 m depth (which corresponds to a potential density of σ_T= 26.4 kg m^{-3}, thus similar to the core density of minimal O_2 concentrations in the eddy).

In addition to metagenomic sampling, carbon uptake measurements were performed during the R/V Meteor M105 survey at two stations: no. 186 (profile 10, 19.3°N, 24.77°W) and no. 190 (profile 15, 18.67°N, 24.87°W, see Fig. 1C, blue crosses).

2.2 Water sampling and Hydrographic parameters

Discrete samples for salinity, dissolved O_2 and nutrients on all surveys were taken from a CTD rosette equipped with Niskin-bottles. The CTD data were calibrated against salinity samples and CTD oxygen probe data (SBE 43 Clark electrode sensor) were calibrated against O_2 concentrations, determined following the Winkler method using 50 or 100 mL samples. Salinity and nutrient concentrations were determined as described in Grasshoff et al. (1999). The CTD on R/V Meteor was equipped with double sensors for conductivity, temperature, and oxygen. Calibration followed standard procedures (GO-SHIP Manual; (Hood et al., 2010)).

2.3 Oxygen respiration

In order to estimate the net O_2 consumption as a potential driver for microbiological community shifts a simple calculation was performed as follows:

(1) $\Delta O_2 = O_2(S) - O_2(E)$

where $O_2(S)$ denotes the lowest O_2 concentration detected on the shelf (36.69 ± 6.91 µmol kg^{-1} at σ_T= 26.3 ± 0.15 kg m^{-3}, cruise M107, average of shelf stations between 18.10°N/ 16.59°W and 18.25°N/ 16.45°W). This region was chosen as it was identified (Schütte et al. (2015), in preparation, this issue) to be the area were the eddy most likely originated. $O_2(E)$ denotes the lowest O_2 concentration measured in the eddy core at the same potential density (4.8 µmol kg^{-1} at σ_T= 26.35 kg m^{-3} during M105).

The daily O_2 loss rate (ΔO_{2d}) was calculated as follows, assuming a lifetime of 180 days of the eddy (Schütte et al. (2015), in preparation, this issue):

(2) $\Delta O_{2d} = \Delta O_2/180$

2.4 Chlorophyll a measurements

Sea water samples (0.5 – 1 L) for chlorophyll *a* (Chl *a*) analyses were filtered (200 mbar) on GF/F filters (25 mm, 0.7 µm; Whatman, Maidstone, UK). Filters were transferred to a plastic vial and 1 mL of MilliQ water was added. Filters were immediately frozen at -20°C and stored for at least 24 h. Afterwards, 9 mL acetone (100 %) was added to the vials and the fluorescence was measured with a Turner Trilogy fluorometer (Sunnyvale, CA, USA). Calibration took place using a Chl *a* standard dilution series (*Anacystis nidulans*, Walter CMP, Kiel, Germany). Chl *a* concentrations were determined as described by Parsons et al. (1984).

2.5 Molecular Methods

Seawater samples were taken from the Niskin-Bottles at selected CTD casts. For nucleic acid purification 2 L seawater was rapidly filtered (exact filtration volumes and times were recorded continuously) through 0.2 µm polyethersulfone membrane filters (Millipore, Billerica, MA, USA). The filters were immediately frozen and stored at −80°C until further analysis. Nucleic acids were purified using the Qiagen DNA/RNA AllPrep Kit (Qiagen, Hilden, Germany) with modifications as previously described (Löscher et al., 2012).

Extracts of DNA and RNA were quantified using a spectrophotometer (Thermo Fisher Scientific, Waltham, MA, USA). To remove DNA from RNA extracts, a DNase I treatment (Invitrogen, Carlsbad,

CA) was performed; purity of RNA was checked by PCR amplification before random reverse transcription with the Quanti Tect® Reverse Transcription Kit (Qiagen, Hilden, Germany). HNLC, HLII and other *Prochlorococcus* ecotypes were qPCR-amplified using primers and PCR conditions as previously described (Ahlgren et al., 2006). Reactions were performed in technical duplicates in a final volume of 12.5 µL using 0.25 µL of each primer (10 pmol μL^{-1}), 3.25 µL nuclease-free water and 6.25 µL SYBR qPCR Supermix W/ROX (Life Technologies, Carlsbad, CA, USA) on a ViiA7 qPCR machine (Life Technologies, Carlsbad, CA, USA) according to established protocols (Ahlgren et al., 2006;West et al., 2011). TaqMan-based qPCRs were performed for picophytoplankton (*Prochlorococcus*/*Synechococcus*) and bacteria as previously described (Suzuki et al., 2001) in a final volume of 12.5 µL with primer/probe concentrations as shown elsewhere (Table 1, (West et al., 2011)), but with the addition of 0.5 µL BSA (20 mg mL^{-1}) and 6.25 µL TaqMan Mix (Life Technologies, Carlsbad, CA, USA). Dilution series of plasmids containing the target gene were used as standards as described (Lam et al., 2007;Löscher et al., 2012). Nitrogen cycle key functional genes *amoA*, *nirS*, *hzo* and *nifH* were amplified and quantified from DNA and cDNA following established protocols (Lam et al., 2007;Langlois et al., 2008;Löscher et al., 2014;Löscher et al., 2012). Detection limits of qPCR assays were determined from no-template controls, which were run in duplicate for each primer (and probe) set, and were undetectable after 45 cycles, thus setting the theoretical detection limit of our assay mixtures to one gene copy. However, detection limits additionally depend on the amount of filtered seawater per sample, elution volume after extraction, and the amount of sample loaded to the qPCR assay. Based on a filtration volume of 2L seawater, a detection limit of 20 copies L^{-1} has been determined. qPCR efficiencies were calculated using the formula $E = 10^{-1/slope} - 1$, and were between 95.3% and 96.8%.

2.5.1 PCR amplification of bacterial and archaeal 16S rDNA for Illumina MiSeq amplicon sequencing

For the analysis of the bacterial community, hypervariable regions V1 and V2 of the 16S rDNA was amplified from genomic DNA using the primer set 27 forward (Frank et al., 2007) and 338 reverse (Fierer et al., 2008). Beside the target-specific region the primer sequence contained a linker sequence, an 8-base barcode and the Illumina specific region P5 (forward primer) or P7 (reverse primer), respectively, as recently described (Kozich et al. 2013). The PCR reaction mixture consisted of 13.6 µL DEPC H_2O (Roth, Karlsruhe, Germany), 0.4 µL of 10 mM dNTPs (Thermo Fisher Scientific), 4 µL 5x HF-buffer (Thermo Fisher Scientific, Waltham, MA, USA), 0.8 µL primers (5 µM, Eurofins, Ebersberg, Germany), 0.2 µL Phusion high fidelity polymerase (2 U μL^{-1}, Thermo Fisher Scientific, Waltham, MA, USA) and 1 µL genomic DNA with a concentration between 10 and 100 ng μL^{-1}. Negative controls consisted of the

reaction mixture as described above without the addition of DNA. PCR reaction conditions started with an initial denaturation step for 5 min at 95°C followed by 30 cycles of 15 s denaturation at 95°C, 30 s primer annealing at 52°C and 30 s elongation at 72°C and a final elongation at 72°C for 5 min.

For analysis of the archaeal community, hypervariable regions V5-V7 of the 16S rDNA were amplified from genomic DNA using the primer set 787 forward and 1059 reverse (Yu et al., 2005) with 8-base barcode and Illumina specific adapters. Reaction mixture, PCR protocol and purification were identical to the amplification of bacterial community DNA amplification, the only difference was the annealing temperature (58°C). Amplification was checked for correct size and band intensity on a 2.5% agarose gel. Amplicons were purified using the MinElute Gel Extraction Kit (Qiagen, Hildesheim, Germany and quantified on a spectrophotometer (Nanodrop 1000, Thermo Fisher Scientific, Waltham, MA, USA). Pooled purified amplicons were prepared and sequenced according to the manufacturer's protocol on a MiSeq Instrument using the MiSeq reagent Kit V3 chemistry (Illumina, San Diego, CA, USA). Sequences were submitted to NCBI Sequence Read Archive under accession number PRJNA288724.

2.5.2 Sequence analysis of 16S rDNA gene amplification

Sequence processing was performed using mothur software version 1.32.1 (Kozich et al., 2013;Schloss et al., 2009). 4,054,723 bacterial sequence read pairs could be concatenated to contiguous sequences (contigs) using the command *make.contig*. Contigs containing ambiguous bases, homopolymers longer than 8 bases or contigs longer than 552 bases were deleted from the dataset. Redundant sequences were clustered using the command *unique.seqs,* which led to 645,444 unique sequences. Sequences were consecutively aligned with *align.seqs* against a modified version of the SILVA database release 102 (Pruesse et al., 2007) containing only the hypervariable regions V1 and V2. The alignment was optimized by removing sequences not aligning in the correct region with *screen.seqs,* and by the removal of gap-only columns using *filter.seqs*. The optimized alignment contained 636,701 sequences of lengths between 255 and 412 bases. Rare sequences with up to 3 positional differences compared to larger sequence clusters were merged with the latter by the *pre.cluster* command. Chimeric sequences were removed with the implemented software UCHIME (Edgar et al., 2011) using the command *chimera.uchime,* followed by *remove.seqs*.

Taxonomic classification of the remaining sequences was done using the Wang approach based on a modified version of the Greengenes database (DeSantis et al., 2006) with a bootstrap threshold of 80%. Sequences of archaea, chloroplasts and mitochondria were removed with *remove.lineage*. Operational taxonomic units (OTUs) were formed by average neighbor clustering using the *cluster.split* command, parallelizing the cluster procedure by splitting the dataset at the taxonomic order level. A sample-by-OTU

table was generated with *make.shared* at the 97 % sequence similarity level. The resulting table contained 15,509 OTUs. OTUs were classified taxonomically using the modified Greengenes database mentioned above and the command *classify.otu*.

Archaeal sequences showed lower quality in the reverse read, which lead to multiple ambiguous bases in the contigs formed. For this reason only the forward read starting from base 36 was used for analysis. Sequence analysis was performed as described above for bacterial 16S sequences, except that the alignment (*align.seqs*) was accomplished using the SILVA archaeal reference release 102 (Pruesse et al., 2007) fitted for hypervariable regions V5-V7.Classification (*classify.seqs* and *classify.otu*) was conducted using the RDP database file release 10 (Cole et al., 2014;Wang et al., 2007). Results and additional information on the archaeal community structure are listed in the supplemental material.
An overview of the sequencing output is given in table S1.

2.6 Statistics

Low-abundance OTUs were removed to reduce noise and computation time. Statistical downstream analysis was performed in R v3.1.3 (R Core Team, 2015) with custom scripts (available from the authors on request). As OTUs of very low abundance only increase computation time without contributing useful information, they were removed from the data set as follows: After transformation of counts in the sample-by-OTU table to relative abundances (based on the total number of reads per sample), OTUs were ordered by decreasing mean percentage across samples. The set of ordered OTUs for which the cumulative mean percentage amounted to 99% was retained in the filtered OTU table.
Distribution of OTUs across samples was modeled by a set of environmental variables (Table S2) with minimal interdependence. The variance in OTU composition (i.e., the extent of change in OTU abundance across samples) explained by the measured environmental variables was explored by redundancy analysis (RDA) with Hellinger-transformed OTU counts (Langfeldt et al., 2014;Stratil et al., 2013;Stratil et al., 2014) using the R package vegan (Oksanen et al., 2013). In order to minimize collinearity of explanatory variables in the RDA model, a subset of the recorded environmental variables was chosen according to their variance inflation factor (VIF), employing vegan's functions *rda* and *vif.cca*. Starting with an RDA model that contained all explanatory variables, the variable with the highest VIF was iteratively determined and removed from the model until all remaining explanatory variables had a VIF <2.5.

OTU distribution was subject to "Realm" depending on O_2 concentration. Model selection started with a full RDA model containing all main effects and possible interactions based on the set of explanatory variables with minimal collinearity. This model was simplified by backward selection with function *ordistep*. The final RDA model exhibited a significant interaction effect "Realm:O_2" (see results section).

For plotting and indicator analysis (see below), the continuous variable "O_2" was converted into a factor with two levels "high O_2" (>90 µmol L^{-1}) and "low O_2" (≤90 µmol L^{-1}); the threshold of 90 µmol L^{-1} was chosen for two reasons: (1) to obtain sample groups of fairly equal size between stations, which include low O_2 parts of the water column at all sampling stations in order to enable a comparison between the ETNA OMZ (outside the eddy) and the eddy OMZ. (2) 90 µmol L^{-1} has previously described the highest concentration of O_2 at which denitrification has been detected to be active (Gao et al., 2010). The presence of *nirS* transcripts (see section 3.4) indicated a potential importance for denitrifiers in the eddy, therefore the theoretical upper limit of 90 µmol L^{-1} was chosen.

We determined OTUs typical for a given combination of levels of factors "Realm" and "O_2". OTUs significantly correlated with any axis in the final RDA model were determined using the function *envfit* with 10^5 permutations, followed by Benjamini-Hochberg correction (false discovery rate, FDR) (Benjamini and Hochberg, 1995). In order to reduce the number of tests in this procedure, OTUs were pre-filtered according to their vector lengths calculated from corresponding RDA scores (scaling 1) by profile likelihood selection (Zhu and Ghodsi, 2006).

OTUs significant at an FDR of 5% were further subject to indicator analysis with function *multipatt* of the R package indicspecies v1.7.4 (De Cáceres and Legendre, 2009) with 10^5 permutations. Indicator OTUs – in analogy to indicator species *sensu* De Cáceres and Legendre (2009) – are OTUs that prevail in a certain sample group (here: a level of factor "Realm" within a chosen O_2 level) while being found only irregularly and at low abundance in other sample groups. In order to remove the effects of the covariate "Depth" in indicator analysis, Hellinger-transformed counts of significant OTUs were first subjected to a linear regression with "Depth"; residuals of this regression were then transformed to positive values by subtraction of their minimum and used as input for indicator analysis.

3D visualizations of the RDA model were produced in kinemage format (Richardson and Richardson, 1992) using the R package R2Kinemage developed by S.C.N., and displayed in KiNG v2.21 (Chen et al., 2009).

Diversity within samples was related to environmental variables by advanced linear regression. For alpha diversity analysis, effective OTU richness (Shannon numbers equivalent, ^1D, (Jost, 2006, 2007)) was calculated from the filtered OTU table. ^1D was fitted to the set of explanatory variables with minimal collinearity in a generalized least squares (GLS) model using function *gls* of the R package nlme v3.1-120 (Pinheiro et al., 2015). The variable "NO2" was square root-transformed to decrease the potential leverage effect of its two highest values (0.25 µmol L^{-1} and 0.28 µmol L^{-1}, respectively) on ^1D. Apart from main

effect terms, the interaction term "Realm:O_2" was included into the GLS model for comparability with beta diversity analysis (see results section). The variance structure of the GLS model was chosen to account for both different variances per level of "Realm" and an overall decreasing variance by "Depth". The resulting model was validated following the recommendations of Zuur et al. (2009). While only the "Realm" effect was significant, the other terms were kept in the model to maintain a valid residual distribution. For visualization of the (partial) effect of only factor "Realm" on ^{1}D, partial response residuals were extracted from the full GLS model re-fitted without the "Realm" main effect. These partial response residuals were then modelled by the "Realm" main effect alone, using the same variance structure as for the full GLS model.

2.7 Carbon fixation rate measurements

Seawater incubations were performed in triplicate at two stations, one inside the eddy (station 10, M105 cruise) and one in ETNA open waters (station 15, M105 cruise, both stations indicated in Fig. 1C). Seawater was sampled from a CTD system and directly filled into 2.8 L polycarbonate bottles (Nalgene, Thermo Fisher Scientific, Waltham, MA, USA). For carbon fixation measurements, $NaH^{13}CO_3$ (Cambridge Isotope Laboratories, MA, USA) was dissolved in sterile deionized water (>18.2 MΩ cm^{-1}, MilliQ, Merck-Millipore, Darmstadt, Germany; 5 g/294 mL). A volume of 1 ml (2.8 L bottles) was added to the incubations with a syringe (~4.4 atom % final). After amendment, bottles were stored on deck in a seawater-cooled Plexiglas incubator covered with light foils (blue-lagoon, Lee filters, Andover, Hampshire, UK) that mimic light intensities at corresponding sampling depths (5/10/30/70 m). Samples from below the euphotic zone were stored at 12°C in the dark. The depth of the euphotic zone was estimated from photosynthetically active radiation (PAR) sensor measurements from CTD profiles as the depth where PAR is <1% of the surface value. This corresponded to 60 m water depth during this survey. After 24 h of incubation, 1.5–2.8 L of seawater were filtered onto pre-combusted (450°C, 5 h) 25 mm diameter GF/F filters (Whatman, Maidstone, UK) under gentle vacuum (-200 mbar). Filtrations were stopped after 1 h since high particle load of surface water led to a clogging of the filters. Filters were oven dried (50°C) for 24 h and stored over desiccant until analysis. Environmental samples of 2.8 L untreated seawater were filtered and prepared in the same way to serve as blank values. For isotope analysis, GF/F filters were acidified over fuming HCl overnight in a desiccator. Filters were then oven-dried for 2 h at 50°C and pelletized in tin cups. Samples were analysed for particulate organic carbon and nitrogen (POC and PON) and isotopic composition using a CHN analyser coupled to an isotope ratio mass spectrometer.

3 Results and Discussion

3.1 Hydrography of low-O_2 eddy reveals similarities to shelf waters

As the detailed properties of the investigated eddy are described in Schütte et al. (2015, in preparation for this issue) only the main characteristics are mentioned here:

The surveyed low-O_2 eddy belongs to the group of the anticyclonic modewater eddies (ACME) (Karstensen et al. 2015a). It has been reported that ACME promote intense primary production in surface and mixed layer waters (Mahadevan, 2014) fueled by nutrient supply to the euphotic zone. The surveyed eddy had a diameter of about 100 km and was characterized by highly elevated mixed layer chlorophyll a (chl*a*) concentrations, a positive SLA signature (Fig. 1) and a low O_2/ low salinity core (Fig. 2). The O_2-depleted core, with concentrations of less than 5 µmol kg^{-1}, was centered rather deep for an ACME at ~100 m depth. Concentrations of less than 30 µmol kg^{-1} were observed in the eddy water column between 70 to 150 m depth (Fig. 2, 3A), which is significantly below average O_2 concentrations in that region,. O_2 concentrations in the core decreased over the survey period (March 2014), (see Fiedler et al. (2015) in this issue, for a detailed description of O_2 properties). During the metagenomic sampling of the background signal ("no eddy") on the shelf (Meteor M107 cruise station 675, 18.22°N/ 16.56°W, Fig. 1), O_2 concentrations of 33.9 µmol kg^{-1} were observed at 115 m depth, which corresponds to the potential density layer of the low O_2 core in the eddy. The open ocean background minimum O_2 concentrations of about 70 µmol kg^{-1} were detected at ~250 m depth at CVOO (Fig. 1). This can be considered average O_2 concentrations for the open ETNA (Karstensen et al., 2008).

In the low-O_2 eddy core, we observed nitrate and phosphate concentrations around twice as high as background concentrations at CVOO at the same depth (Fig. 3). However, N:P ratios below the mixed layer were close to Redfield stoichiometry (16.15 ± 0.63, Fig. 3) and thus comparable to surrounding waters. Nitrate concentrations in the O_2-min core (~100 m depth) were similar to concentrations on the Mauritanian shelf at 100 m depth (Fig. 3) and most likely generated by very efficient local remineralization of nitrate from the sinking material (Karstensen et al. 2015b, in preparation for this issue).

3.2 Loss of phylogenetic diversity in low-O_2 eddy waters

A critical issue regarding climate change induced pressures on ocean ecosystems is to understand the effects of ocean acidification and deoxygenation on microbial communities as major drivers of the ocean's biogeochemistry (Riebesell and Gattuso, 2015). Thus, we investigated phylogenetic diversity of the microbial community with a 16S rDNA amplicon sequencing approach of bacteria and archaea inside and outside the eddy.

Although the bacterial community was dominated by Proteobacteria in all samples, there were distinct differences between the community structures inside compared to outside the eddy (Fig. 4). Increased

abundances of the uncultivated SUP05 clade (up to 20% of proteobacterial sequences), have been recovered from eddy samples compared to surrounding waters (Fig S1, Table S3). This clade is known to occur frequently in O_2 depleted environments (Swan et al., 2011). Phyla such as Bacteroidetes, Actinobacteria and Firmicutes were only present in the eddy and increased in relative abundance over time. Those phyla were also detected in potential source waters on the shelf (Fig. S2). Interestingly, the family of Pelagibacteraceae, which belong to the ubiquitous SAR11 clade (Giovannoni et al., 1990), were strongly decreased in the eddy (to ~1% of all reads), compared to CVOO samples (~65% of all reads). SAR11 was previously described as being sensitive to decreasing O_2 concentrations (Forth et al., 2014), which may explain the absence of this classically highly abundant group from the eddy. In addition to the dissimilarity in bacterial diversity, we also detected a substantial difference in archaeal community composition between eddy stations and CVOO (Fig. S3). This was most obvious in samples from the eddy_2 station, where Methanomicrobia dominated the archaeal community in the O_2-depleted parts of the water column but was absent in CVOO samples. The presence of methanogens in the low-O_2 eddy core samples may indicate potential for methanogenesis. Although the eddy has not been shown to become fully anoxic, methanogenesis tolerates O_2 concentrations at low ranges (Angel et al., 2011).

Redundancy analysis (RDA) confirmed that the distribution of bacterial OTUs strongly differed between the two eddy stations and CVOO samples (Fig. 6A; RDA model: $F_{6,24} = 4.48$, $p<.001$). Changes in OTU composition mirrored the depth gradient (RDA "Depth": $F_{1,24} = 2.08$, $p\approx .03$; Fig. 5) and were thus strongly correlated to chemical (PO_4^{3-}, NO_3^-, SiO_2) and physical (T, S) properties (Fig. S4). The RDA model indicates a noticeable interaction effect of habitat ("Realm") and O_2 concentration (RDA "Realm:O_2": $F_{2,24} = 2.03$, $p\approx .02$), meaning that the "Realm" effect on bacterial community structure depends on the O_2 level and vice versa. An overview of the parameters included in the RDA model is given in table S2. O_2 and nutrient availability can thus be considered the major determining variables for the composition of the microbial community.

Our results show further a significant decrease in bacterial alpha diversity in the eddy relative to CVOO (Fig. 6). The community in eddy_2 samples was also markedly less diverse compared to those of the other realms (Fig. 6; generalized least squares (GLS) model: $F_{7,23} = 5.37$, $p = .001$; GLS "Realm": $F_{2,23} = 16.26$, $p<.0001$). This may be attributed to an aging effect of the eddy, and corresponds to progressive O_2 loss and consecutive changes in the eddy biogeochemistry. We calculated an overall O_2 loss of 0.18 µmol kg^{-1} d^{-1} at 100 m depth by respiration, when comparing the eddy core water to the potential origin waters on the shelf, assuming a lifetime of 180 days for the eddy (average O_2 concentrations on the shelf from Meteor M107 were 36.69 ± 6.91 µmol kg^{-1} compared to observed minimum O_2 concentrations of 4.8 µmol kg^{-1} in the eddy core). These results are comparable to previous estimates on low O_2-eddies in that region (Karstensen et al., 2015a). Likewise, Fiedler et al. (2015) also observed a significant increase in pCO_2 and dissolved inorganic carbon compared to coastal waters, indicating enhanced remineralization and

407 respiration. Although our dataset does not allow differentiation between high-pCO_2 and low-O_2 effects on
408 the microbial community, it supports the view of a general loss in diversity. This may be attributed to a
409 direct or indirect response to factors related to deoxygenation and increasing pCO_2, such as the impact on
410 nutrient stoichiometry, as previously suggested (Bryant et al., 2012).
411 Hence, climate change-related ocean deoxygenation and consequent shifts in nutrient stoichiometry may
412 mean an overall loss of microbial diversity, with potential for substantial loss in the spectrum of metabolic
413 functions in the future ocean.
414
415 ### 3.3 Specific *Prochlorococcus* clade contributes to primary production in the eddy
416 The detected ACME was characterized by shoaling of the mixed layer depth in the center of the eddy.
417 This coincided with a pronounced surface chl*a* maximum as observed by ocean color based and remotely
418 sensed chl*a* estimates (Fig. 1a, Fig. 7), which was slightly deeper (~50-70 m water depth) outside the
419 eddy. In accordance with increased chl*a* concentrations, enhanced carbon uptake was observed via direct
420 rate measurements of $H^{13}CO_3^-$ uptake which was potentially fueled by increased nutrient availability from
421 intermediate depths. We found a 3-fold increase in depth-integrated carbon uptake rate in the chl*a*
422 maximum of the eddy (178.3 ± 30.8 m mol C m^{-2} d^{-1}) compared to surrounding waters (59.4 ± 1.2 mmol C
423 m^{-2} d^{-1}).
424 While the upper chl*a* maximum in the eddy may likely be ascribed to eukaryotic primary producers such
425 as diatoms and flagellates that are widely distributed and abundant in that region (Franz et al., 2012),
426 confirmed by increased abundances of plastids in surface samples of our amplicon dataset (Table S3). A
427 secondary chl*a* maximum dominated by cyanobacteria was detected in the eddy at about 100 m water
428 depth, coinciding with the O_2 minimum.
429 The quantitative analysis of cyanobacterial primary producers by 16S rDNA-qPCR further revealed
430 dominance of a specific clade of *Prochlorococcus* in the secondary chl*a* maximum (Fig. S5 depicts
431 phylogenetic relations of detected *Prochlorococcus* clades). This ecotype has so far not been identified in
432 the ETNA and is only known from high nutrient low chlorophyll (HNLC) regions of the eastern tropical
433 Pacific Ocean (West et al., 2011). Its described adaptation to high nutrient conditions such as present in
434 this O_2-depleted ACME points towards a selective advantage for this clade. Gene abundance of this
435 ecotype—for convenience further referred to as HNLC-PCC (results of an ecotypespecific16S rDNA
436 based qPCR)— showed a strong correlation with chlorophyll (R^2= 0.95, n=22) below the euphotic zone
437 within the eddy. This correlation was not present outside the eddy, where HNLC-PCC abundance was
438 approximately one third compared to the second eddy observation (Fig. 8). The *Prochlorococcus*
439 community in surrounding waters was, however, dominated by another high-light ecotype of
440 *Prochlorococcus* (further referred to as HL-PCC (West et al., 2011)). Contrary to HNLC-PCC, HL-PCC
441 was not detected inside the eddy. The difference between the CVOO, eddy_1 and eddy_2 observations

points towards a community shift of *Prochlorococcus* related clades depending on specific characteristics of the eddy (O_2, nutrient availability) with the potential to alter primary productivity in that region. Under increasing pCO_2 levels, *Prochlorococcus* is predicted to substantially increase in abundance (Flombaum, 2013). Elevated pCO_2 levels in the eddy core water may therefore—apart from favorable elevated nutrient concentrations—explain the additional selective advantage of specific *Prochlorococcus* clades, in this case of HNLC-PCC. This may be critical as *Prochlorococcus* is one of the most abundant photosynthetic organisms in the ocean and contributes to ~40% of dissolved organic carbon supporting bacterial production (Bertillson et al., 2005).

Besides a direct impact of O_2, nutrients and pCO_2, increased abundances of *Prochlorococcus* in the eddy may be explained from an interaction effect in the microbial community present in the eddy. *Prochlorococcus* is supposed to play a major role in sustaining heterotrophs with organic carbon compounds such as glycine and serine, thus favoring their growth (Biller et al., 2015;Carini et al., 2013). Conversely, *Prochlorococcus* benefits from the presence of heterotrophs as they diminish the concentration of reactive oxygen species in their immediate surroundings, which is not feasible for *Prochlorococcus* due to the lack of catalase and peroxidase genes (Berube et al., 2014;Morris et al., 2008). The close proximity of increased abundances of the HNLC-PCC maximum to the O_2 minimum in the eddy may thus point towards a beneficial relationship between the HNLC-PCC and the heterotroph-dominated, eddy core water microbial community.

3.4 Increased primary productivity promotes a specific heterotrophic microbial community in underlying waters

We analyzed species indicative for the eddy and CVOO for either high-O_2 conditions (>90 µmol kg^{-1}) or low-O_2 conditions (≤90 µmol kg^{-1}). Indicator OTUs for high O_2 in the eddy were mostly associated with different clades of Proteobacteria, whereas Pelagibacteraceae dominated at CVOO in accordance with several studies describing those organisms as ubiquitous in open-ocean oxic waters (Morris et al., 2002;Rappé et al., 2002);(Poretsky et al., 2009;DeLong, 2009;Brown et al., 2014). High-O_2 samples of all three sampling stations were dominated - as most parts of the ocean - by indicator OTUs belonging to the Proteobacteria. The *Prochlorococcus* clade HNLC-PCC targeted by qPCR could be recovered in the 16S rDNA amplicon sequences, as well.

For low-O_2 conditions, indicator species present in the eddy were mostly affiliated to the Cytophaga-Flavobacteria-Bacteroides (CFB) group (Glöckner et al., 1999) (Table S4). Members of Bacteroidetes and Proteobacteria (*Gramella, Leeuwenhoekiella marinoflava*, unclassified Comamonadaceae species) were found to be indicative for the low-O_2 realm. *Gramella*-like organisms are usually a quantitatively important fraction of the heterotrophic marine bacterioplankton, often attached to marine snow but also found free-living in nutrient-rich microenvironments (Buchan et al., 2014). Frequently associated with

extensive phytoplankton blooms (Buchan et al., 2014), their ability to degrade high molecular weight compounds in both the dissolved and particulate fraction of the marine organic matter pool points towards a specific role in respiration processes and the marine C cycle (as described for '*Gramella forsetii*' KT0803, Bauer et al. (2006). Karstensen et al. (2015a) described a particle maximum associated to the low-O_2 core of those eddies which likely harbors this specific heterotrophic community. Further, in the core of the ACME presented here, the integrated abundance (upper 600 m) of large aggregates was five times higher than in surrounding waters (Hauss et al., 2015).

Enhanced productivity and consecutive respiration and O_2 decrease may enable N loss processes to occur in the open ETNA, which have previously not been described for the ETNA waters (Löscher et al., 2015;Löscher et al., 2012;Ryabenko et al., 2012). qPCR results of key gene distribution (*amoA* for nitrification as sum of bacterial and archaeal nitrifiers, *nirS* as key gene for denitrification) in that area show a decrease of *amoA* in the eddy, while *nirS* shows higher abundances inside the eddy with ~3000 copies L^{-1} at depth of the O_2 minimum (compared to ~100 copies L^{-1} outside the eddy). Besides a direct sensitivity of nitrifiers to anoxic conditions, the decrease in *amoA* gene abundance (determined by qPCR) towards the O_2 minimum in the eddy may result from an effect of elevated pCO_2 (see Fiedler et al. (2015), this issue) and the corresponding drop in pH on ammonia due to a shift in the ammonia/ammonium equilibrium. The latter has previously been described to alter the efficiency of nitrification (Beman et al., 2011). Further, *nirS* transcripts as quantified by qPCR were detected in abundances up to 3600 transcripts L^{-1} in the eddy O_2 minimum, while no transcripts were detected outside the eddy (Fig. 9).

The presence and expression of *nirS* supports the view that potential for N loss is also present in the usually oxic open ETNA. This is in line with another study on nitrous oxide (N_2O) production from the same eddy (Grundle et al., submitted), where the authors observed massively increased N_2O concentrations in the oxygen deficient eddy core waters in connection with denitrification. Observations from e.g. the eastern tropical Pacific Ocean demonstrated previously that mesoscale eddies are drifting hotspots of N loss (Altabet et al., 2012). This might be explained by feedback mechanisms between eutrophication, enhanced primary productivity and consecutive enhanced export production, which may promote denitrification in those systems as suggested by Kalvelage et al. (2013). Our results strongly suggest that N loss is possible in eddy systems of that region, thus altering one major biogeochemical cycle with unknown consequences for the ETNA biogeochemistry.

In case of the described eddy, we neither detected key genes for anammox (*hzo*, Schmid et al. (2008)) nor significant abundances of the key genes for dinitrogen fixation. The latter has been investigated by screening for the functional key gene, *nifH*, which has been tested for classical diazotrophs as *Trichodesmium*, UCYN-A, UCYN-B, UCYN-C, gamma proteobacterial diazotrophs and DDAs; all of

512 which were not quantifiable by qPCR. This may be explained by the high availability of inorganic N
513 sources, as well as the prevalence of N:P close to the Redfield ratio of 16:1 as mentioned above.
514 Although N_2 fixation does not appear to play a role in the low-oxic core waters or adjacent surface waters
515 of the eddy, it may occur as a result of increasing N loss and resulting excess P as previously discussed for
516 other O_2 depleted marine habitats (Deutsch et al., 2007;Fernandez et al., 2011;Löscher et al., 2014;Ulloa et
517 al., 2012).
518

519 ## 4 Conclusions

520 We investigated the microbial community structure and gene expression in a severely O_2-depleted
521 anticyclonic modewater eddy in the open waters of the ETNA OMZ region. This was then compared the
522 eddy observations to background signals from the ETNA open ocean CVOO time series site and the
523 Mauritanian upwelling region, where the eddy was likely formed.
524 A significant difference between microbial communities outside and inside the eddy along with an overall
525 loss in bacterial diversity in the low-O_2 core of the eddy was observed. Similarity was found between the
526 microbial community in the eddy core and on the shelf. This unique microbial community may shape the
527 specific character of this O_2-depleted eddy progressively over time.
528 We observed enhanced primary production in the eddy, presumably due to an increased nutrient supply
529 related to the eddy dynamics (Karstensen et al. 2015b). We found a specific HNLC ecotype of
530 *Prochlorococcus*, which may play a role in mediating inorganic C to certain organic C sources for the
531 associated heterotrophic community present in the eddy. Importantly, we found the first indication for N
532 loss processes in the ETNA region. Low-O_2 eddies in that region thus represent an isolated ecosystem in
533 the open ocean, forced by strongly elevated biological productivity, which travels with the eddy. This
534 leads to consequent enhanced respiration and further deoxygenation in its core waters.
535 At one stage the low-O_2 eddies will lose coherence and the extreme signatures will be released into and
536 mixed with the surrounding waters (Karstensen et al. 2015a). The ACME formation frequency for the
537 ETNA (12°-22°N and 15°-26°W) has been estimated to be about 2 to 3 yr^{-1} (Schütte et al. 2015, in
538 preparation for this issue), hence no large scale impact of the eddies are expected. However, an
539 unexpected shift in elemental ratios or other anomalies, normally expected for regions with much lower
540 minimal oxygen levels than the ETNA, may be detected and explained by the dispersal of low-O_2 eddies.
541 Another factor to consider is the impact of deoxygenation of the ETNA (Stramma et al., 2008) as it may
542 result in even lower O_2 conditions to be created in the low-O_2 eddies. With regard to the distinct character
543 of the low-O_2 eddies and the critical shift in microbial diversity and biogeochemistry that occur over
544 relatively short times, this study contributes to understand and evaluate the far-reaching effects of future
545 and past ocean deoxygenation.
546

Author contribution

C.R.L. designed the study together with B.F., A.K., H.H. and J.K.; M.P. and C.R.L. validated the NGS primer sets for marine samples, performed the molecular analysis, processed the molecular data and analyzed hydrographic data. S.K. performed the high-throughput sequencing runs. M.A.F. and S.C.N. performed bioinformatic analysis of high-throughput datasets. A.S. performed C-uptake measurements and data analysis, F.S., J.K. and A.K. designed the eddy detection and tracking system. B.F., F.S., A.K., H.H. and C.R.L. planned the sampling campaign and B.F. performed hydrographical measurements and analyzed the data. S.C.N. performed statistical analysis and modeling. C.R.L. wrote the manuscript with input from all co-authors.

Acknowledgements

We thank the authorities of Cape Verde and Mauritania for the permission to work in their territorial waters. We acknowledge the support of the captains and crews of R/V Islandia and R/V Meteor as well as the chief scientist of M105, M. Visbeck, for his spontaneous support. Moreover, we acknowledge I. Monteiro and M. Lohmann for performing oxygen and nutrient measurements, D. Grundle for sampling on RV Islandia, C. Hoffman for technical assistance and the captains, crews and chief scientists of Meteor M107, S. Sommer and M. Dengler, for providing hydrographical data. We acknowledge H. Bange, G. Krahmann and R. Kiko for helpful discussion of the results. G. Petrick, flying to Cape Verde to repair the liquid N_2 generator was priceless- we thank you a lot for this personal effort! We thank T. Treude for editing this manuscript. Further, we thank J. M. Beman and two anonymous reviewers for helpful discussion of the manuscript and A. Paul for language editing.

Financial support for this study was provided by a grant from the cluster of excellence 'The Future Ocean' to C.R.L., A.K. and H.H.. Authors C.R.L., S.C.N., H.H. and M.P. were funded by the DFG Collaborative Research Centre754 (www.sfb754.de). M.A.F. was funded and S.C.N. was co-funded by the BMBF project BioPara funded to R.A.S (grant no. 03SF0421B), A.S. was funded by the cluster of excellence 'The Future Ocean', B.F. was funded by the BMBF project SOPRAN (grant no. 03F0662A).

References

Ahlgren, N., Rocap, G., and Chisholm, S.: Measurement of Prochlorococcus ecotypes using real-time polymerase chain reaction reveals different abundances of genotypes with similar light physiologies, Environmental Microbiology, 8, 441–454, 2006.

Altabet, M. A., Ryabenko, E., Stramma, L., Wallace, D. W. R., Frank, M., Grasse, P., and Lavik, G.: An eddy-stimulated hotspot for fixed nitrogen-loss from the Peru oxygen minimum zone, Biogeosciences, 9, 4897–4908, 2012.

Angel, R., Matthies, D., and Conrad, R.: Activation of Methanogenesis in Arid Biological Soil Crusts Despite the Presence of Oxygen, PlosOne, 6, doi:10.1371/journal.pone.0020453, 2011.

Arévalo-Martínez, D. L., Kock, A., Löscher, C. R., Schmitz R. A., and Bange, H. W.: Influence of mesoscale eddies on the distribution of nitrous oxide in the eastern tropical South Pacific, Biogeosciences Discuss., 12, 9243-9273, doi:10.5194/bgd-12-9243-2015, 2015.

Baird, M. E., Suthers, I. M., Griffin, D. A., Hollings, B., Pattiaratchi, C., Everett, J. D., Roughan, M., Oubelkheir, K., and Doblin, M.: The effect of surface flooding on the physicalâ€“biogeochemical dynamics of a warm-core eddy off southeast Australia, Deep Sea Research Part II: Topical Studies in Oceanography, 58, 592-605, 2011.

Bauer, M., Kube, M., Teeling, H., Richter, M., Lombardot, T., Allers, E., Würdemann, C. A., Quast, C., Kuhl, H., Knaust, F., Woebken, D., Bischof, K., Mussmann, M., Choudhuri, J. V., Meyer, F., Reinhardt, R., Amann, R. I., and Glöckner, F. O.: Whole genome analysis of the marine Bacteroidetes'Gramella forsetii' reveals adaptations to degradation of polymeric organic matter, Environ Microbiol. , 8, 2201-2213, 2006.

Beman, J. M., Chow, C. E., King, A. L., Feng, Y. Y., Fuhrman, J. A., Andersson, A., Bates, N. R., Popp, B. N., and Hutchins, D. A.: Global declines in oceanic nitrification rates as a consequence of ocean acidification, Proc. Natl. Acad. Sci. U. S. A., 108, 208-213, 10.1073/pnas.1011053108, 2011.

Beman, J. M., and Carolan, M. T.: Deoxygenation alters bacterial diversity and community composition in the ocean's largest oxygen minimum zone, Nature Communications, 4, doi:10.1038/ncomms3705, 2013.

Benjamini, Y., and Hochberg, Y.: Controlling the false discovery rate: A practical and powerful approach to multiple testing, Journal of the Royal Statistical Society: Series B (Statistical Methodology), 57, 289-300, 1995.

Bertillson, S., Berglund, O., Pullin, M. J., and Chisholm, S. W.: Release of dissolved organic matter by Prochlorococcus, ie et milieu - Life and environment 55, 225-231, 2005.

Berube, P. M., Biller, S. J., Kent, A. G., Berta-Thompson, J. W., Roggensack, S. E., Roache-Johnson, K. H., Ackerman, M., Moore, L. R., Meisel, J. D., Sher, D., Thompson, L. R., Campbell, L., Martiny A., and Chisholm, S. W.: Physiology and evolution of nitrate acquisition in Prochlorococcus, ISME J, http://dx.doi.org/10.1038/ismej.2014.211, 2014.

612 Biller, S. J., Berube, P. M., Lindell, D., and Chisholm, S. W.: Prochlorococcus: the structure and
613 function of collective diversity, Nat Rev Micro, 13, 13-27, 2015.

614 Brown, M. V., Ostrowski, M., Grzymski, J. J., and Lauro, F. M.: A trait based perspective on the
615 biogeography of common and abundant marine bacterioplankton clades, Marine Genomics, 15,
616 17-28, 2014.

617 Bryant, J. A., Stewart, F. J., Eppley, J. M., and DeLong, E. F.: Microbial community phylogenetic
618 and trait diversity declines with depth in a marine oxygen minimum zone, Ecology, 93, 1659-
619 1673, 2012.

620 Buchan, A., LeCleir, G. R., Gulvik, C. A., and González, J. M.: Master recyclers: features and
621 functions of bacteria associated with phytoplankton blooms, Nat Rev Microbiol. , 12, 686-698,
622 doi: 10.1038/nrmicro3326, 2014.

623 Carini, P., Steindler, L., Beszteri, S., and Giovannoni, S. J.: Nutrient requirements for growth of
624 the extreme oligotroph 'Candidatus Pelagibacter ubique' HTCC1062 on a defined medium, ISME
625 J, 7, 592–602, 2013.

626 Chavez, F. P., and Messié, M.: A comparison of Eastern Boundary Upwelling Ecosystems,
627 Progress in Oceanography, 83, 80-96, 2009.

628 Chelton, D. B., Gaube, P., Schlax, M. G., Early, J. J., and Samelson, R. M.: The Influence of
629 Nonlinear Mesoscale Eddies on Near-Surface Oceanic Chlorophyll, Science, 334, 328–332,
630 2011.

631 Chen, V. B., Davis, I. W., and Richardson, D. C.: KING (Kinemage, Next Generation): A versatile
632 interactive molecular and scientific visualization program, Prot Sci, 18, 2403-2409,
633 10.1002/pro.250, 2009.

634 Cole, J. R., Wang, Q., Fish, J. A., Chai, B., McGarrell, D. M., Sun, Y., Brown, C. T., Porras-
635 Alfaro, A., Kuske, C. R., and Tiedje, J. M.: Ribosomal Database Project: data and tools for high
636 throughput rRNA analysis, Nucleic Acids Res., 42, 633-642, doi: 10.1093/nar/gkt1244, 2014.

637 De Cáceres, M., and Legendre, P.: Associations between species and groups of sites: indices
638 and statistical inference, Ecology, 90, 3566-3574, 10.1890/08-1823.1, 2009.

639 DeLong, E. F.: The microbial ocean from genomes to biomes, Nature, 459, 200-206,
640 10.1038/nature08059, 2009.

641 DeSantis, T. Z., Hugenholtz, P., Larsen, N., Rojas, M., Brodie, E. L., Keller, K., Huber, T., Dalevi,
642 D., Hu, P., and Andersen, G. L.: Greengenes, a chimera-checked 16S rRNA gene database and
643 workbench compatible with ARB, Applied and environmental microbiology, 72, 5069–5072,
644 10.1128/aem.03006-05, 2006.

645 Deutsch, C., Sarmiento, J. L., Sigman, D. M., Gruber, N., and Dunne, J. P.: Spatial coupling of
646 nitrogen inputs and losses in the ocean, Nature, 445, 163-167, 10.1038/nature05392, 2007.

647 Edgar, R. C., Haas, B. J., Clemente, J. C., Quince, C., and Knight, R.: UCHIME improves
648 sensitivity and speed of chimera detection, Bioinformatics 27, d2194–2200,
649 10.1093/bioinformatics/btr381, 2011.

650 Fernandez, C., Farias, L., and Ulloa, O.: Nitrogen Fixation in Denitrified Marine Waters, Plos
651 One, 6, 9, e20539,10.1371/journal.pone.0020539, 2011.

652 Fiedler, B., Grundle, D., Hauss, H., Krahmann, G., Schütte, F., Monteiro, I., Silva, P., Vieira, N.,
653 and Körtzinger, A.: Biogeochemistry of oxygen depleted mesoscale Eddies in the open eastern
654 tropical North Atlantic In prep for Biogeosciences Discussion, 2015.

655 Fierer, N., Hamady, M., Lauber, C. L., and Knight, R.: The influence of sex, handedness, and
656 washing on the diversity of hand surface bacteria, Proc. Natl. Acad. Sci. U. S. A., 105, 17994–
657 17999, 10.1073/pnas.0807920105, 2008.

658 Fischer, G., Karstensen, J., Romero, O., Baumann, K.-H., Donner, B., Hefter, J., Mollenhauer,
659 G., Iversen, M., Fiedler, B., Monteiro, I., and Körtzinger, A.: Bathypelagic particle flux signatures
660 from a suboxic eddy in the oligotrophic tropical North Atlantic: production, sedimentation and
661 preservation, Biogeosciences Discuss., 12, 18253-18313, 10.5194/bgd-12-18253-2015, 2015.

662 Flombaum, P., et al. : Present and future global distributions of the marine Cyanobacteria
663 Prochlorococcus and Synechococcus, Proc. Natl. Acad. Sci. USA., 110, 9824–9829, 2013.

664 Forth, M., Liljebladh, B., Stigebrandt, A., Hall, P. O. J., and Treusch, A. H.: Effects of ecological
665 engineered oxygenation on the bacterial community structure in an anoxic fjord in western
666 Sweden, ISME Journal, 9, DOI: 10.1038/ismej.2014.172 2014.

667 Frank, D. N., St Amand, A. L., Feldman, R. A., Boedeker, E. C., Harpaz, N., and Pace, N. R.:
668 Molecular-phylogenetic characterization of microbial community imbalances in human
669 inflammatory bowel diseases, Proc. Natl. Acad. Sci. U. S. A., 104, 13780–13785,
670 10.1073/pnas.0706625104, 2007.

671 Franz, J. M. S., Hauss, H., Sommer, U., Dittmar, T., and Riebesell, U.: Production, partitioning
672 and stoichiometry of organic matter under variable nutrient supply during mesocosm
673 experiments in the tropical Pacific and Atlantic Ocean, Biogeosciences, 9, 4629-4643, 2012.

674 Ganesh, S., Parris, D. J., DeLong, E. F., and Stewart, F. J.: Metagenomic analysis of size-
675 fractionated picoplankton in a marine oxygen minimum zone, ISME J, 8, 187-211, 2014.

676 Gao, H., Schreiber, F., Collins, G., Jensen, M. M., Kostka, J. E., Lavik, G., de Beer, D., Zhou, H.-
677 Y., and Kuypers, M. M. M.: Aerobic denitrification in permeable Wadden Sea sediments, ISME J,
678 4, 417-426, 2010.

679 Giovannoni, S. J., Britschgi, T. B., Moyer, C. L., and Field, K. G.: Genetic diversity in Sargasso
680 Sea bacterioplankton, Nature, 345, 60–63, doi:10.1038/345060a0, 1990.

681 Glöckner, F. O., Fuchs, B. M., and Amann, R.: Bacterioplankton compositions of lakes and
682 oceans: a first comparison based on fluorescence in situ hybridization, Environ Microbiol., 65,
683 3721–3726, 1999.

684 Grasshoff, G., Kremling, K., Erhardt, M. : Methods of seawater analysis, 3 ed., Wiley VCH,
685 Weinheim, 1999.

686 Grundle, D. S., Löscher, C. R., Krahmann, G., Altabet, M. A., Bange, H. W., Karstensen, J.,
687 Körtzinger, A., and Fiedler, B.: Extreme N_2O activity in an oxygenated ocean, submitted.

688 Hauss, H., Christiansen, S., Schütte, F., Kiko, R., Edvam Lima, M., Rodrigues, E., Karstensen,
689 J., Löscher, C. R., Körtzinger, A., and Fiedler, B.: Dead zone or oasis in the open ocean?
690 Zooplankton distribution and migration in low-oxygen modewater eddies, Biogeosciences
691 Discuss., 12, 18315-18344, doi:10.5194/bgd-12-18315-2015, 2015.

692 Hood, E. M., Sabine, C. L., and Sloyan, B. M.: The GO-SHIP Repeat Hydrography Manual: A
693 Collection of Expert Reports and Guidelines, 2010.

694 Jickells, T. D., An, Z. S., Andersen, K. K., Baker, A. R., Bergametti, G., Brooks, N., Cao, J. J.,
695 Boyd, P. W., Duce, R. A., Hunter, K. A., Kawahata, H., Kubilay, N., laRoche, J., Liss, P. S.,
696 Mahowald, N., Prospero, J. M., Ridgwell, A. J., Tegen, I., and Torres, R.: Global iron
697 connections between desert dust, ocean biogeochemistry, and climate, Science, 308, 67-71,
698 2005.

699 Jost, L.: Entropy and diversity, Oikos, 113, 363-375, DOI 10.1111/j.2006.0030-1299.14714.x,
700 2006.

701 Jost, L.: Partitioning diversity into independent alpha and beta components, Ecology, 88, 2427-
702 2439, 10.1890/06-1736.1, 2007.

703 Kalvelage, T., Lavik, G., Lam, P., Contreras, S., Artega, L., Löscher, C. R., Oschlies, A.,
704 Paulmier, A., Stramma, L., and Kuypers, M. M. M.: Nitrogen cycling driven by organic matter
705 export in the South Pacific oxygen minimum zone, Nature Geosci, 6, 228-234, 2013.

706 Karstensen, J., Stramma, L., and Visbeck, M.: Oxygen minimum zones in the eastern tropical
707 Atlantic and Pacific oceans, Progress in Oceanography, 77, 331-350,
708 10.1016/j.pocean.2007.05.009, 2008.

709 Karstensen, J., Fiedler, B., Schütte, F., Brandt, P., Körtzinger, A., Fischer, G., Zantopp, R.,
710 Hahn, J., Visbeck, M., and Wallace, D.: Open ocean dead-zone in the tropical North Atlantic
711 Ocean, Biogeosciences Discussion, 12, 2597-2605, doi:10.5194/bg-12-2597-2015, 2015a.

712 Karstensen, J., Schütte, F., Pietri, A., Krahmann, G., Fiedler, B., Körtzinger, A., Löscher, C. R.,
713 Grundle, D., and Hauss, H.: Anatomy of open ocean dead-zones based on high-resolution
714 multidisciplinary glider data, In prep for Biogeosciences Discussion, 2015b.

715 Kozich, J. J., Westcott, S. L., Baxter, N. T., Highlander, S. K., and Schloss, P. D.: Development
716 of a dual-index sequencing strategy and curation pipeline for analyzing amplicon sequence data
717 on the MiSeq Illumina sequencing platform, Appl. Environ. Microbiol., 79, 5112–5120,
718 10.1128/aem.01043-13, 2013.

719 Lam, P., Jensen, M. M., Lavik, G., McGinnis, D. F., Muller, B., Schubert, C. J., Amann, R.,
720 Thamdrup, B., and Kuypers, M. M. M.: Linking crenarchaeal and bacterial nitrification to
721 anammox in the Black Sea, Proc. Natl. Acad. Sci. U. S. A., 104, 7104-7109,
722 10.1073/pnas.0611081104, 2007.

723 Langfeldt, D., Neulinger, S. C., Heuer, W., Staufenbiel, I., Künzel, S., Baines, J. F., Eberhard, J.,
724 and Schmitz, R. A.: Composition of microbial oral biofilms during maturation in young healthy
725 adults, PlosOne, 9, e87449, 10.1371/journal.pone.0087449, 2014.

726 Langlois, R. J., Hummer, D., and LaRoche, J.: Abundances and distributions of the dominant
727 nifH phylotypes in the Northern Atlantic Ocean, Applied and Environmental Microbiology, 74,
728 1922-1931, 10.1128/aem.01720-07, 2008.

729 Lévy, M., Klein, P., and Treguier, A.-M.: Impacts of sub-mesoscale physics on phytoplankton
730 production and subduction, J. Mar. Res., 59, 535-565, doi: 10.1357/002224001762842181,
731 2001.

732 Lévy, M., Ferrari, R., Franks, P. J. S., Martin, A. P., and Riviere, P.: Bringing physics to life at the
733 submesoscale, Geophysical Research Letters, 39, 10.1029/2012gl052756, 2012.

734 Löscher, C. R., Kock, A., Könneke, M., LaRoche, J., Bange, H. W., and Schmitz, R. A.:
735 Production of oceanic nitrous oxide by ammonia-oxidizing archaea, Biogeosciences 9, 2419-
736 2429, 2012.

737 Löscher, C. R., Großkopf, T., Desai, F., Gill, D., Schunck, H., Croot, P., Schlosser, C., Neulinger,
738 S. C., Lavik, G., Kuypers, M. M. M., LaRoche, J., and Schmitz, R. A.: Facets of diazotrophy in
739 the oxygen minimum zone off Peru, ISME J, 8, 2180-2192, doi: 10.1038/ismej.2014.71, 2014.

740 Löscher, C. R., Bange, H. W., Schmitz R. A., Callbeck, C. M., Engel, A., Hauss, H., Kanzow, T.,
741 Kiko, R., Lavik, G., Loginova, A., Melzner, F., Neulinger, S. C., Pahlow, M., Riebesell, U.,
742 Schunck, H., Thomsen, S., and Wagner, H.: Water column biogeochemistry of oxygen minimum
743 zones in the eastern tropical North Atlantic and eastern tropical South Pacific Oceans
744 Biogeosciences Discussion, 12, 4495-4556, doi:10.5194/bgd-12-4495-2015, 2015.

745 Mahadevan: Ocean science: Eddy effects on biogeochemistry, Nature Geoscience, 506, 168-
746 169, doi:10.1038/nature13048, 2014.

747 McGillicuddy, D. J., Anderson, L. A., Bates, N. R., Bibby, T., Buesseler, K. O., Carlson, C. A.,
748 Davis, C. S., Ewart, C., Falkowski, P. G., Goldthwait, S. A., Hansell, D. A., Jenkins, W. J.,
749 Johnson, R., Kosnyrev, V. K., Ledwell, J. R., Li, Q. P., Siegel, D. A., and Steinberg, D. K.:
750 Eddy/wind interactions stimulate extraordinary mid-ocean plankton blooms, Science, 316, 1021-
751 1026, 10.1126/science.1136256, 2007.

752 Morris, J. J., Kirkegaard, R., Szul, M. J., Johnson, Z. I., and Zinser, E. R.: Facilitation of robust
753 growth of Prochlorococcus colonies and dilute liquid cultures by 'helper' heterotrophic bacteria,
754 Appl. Environ. Microbiol., 74, 4530–4534, 2008.

755 Morris, R. M., Rappé, M. S., Connon, S. A., Vergin, K. L., Siebold, W. A., Carlson, C. A., and
756 Giovannoni, S. J.: SAR11 clade dominates ocean surface bacterioplankton communities, Nature
757 420, 806-810, doi:10.1038/nature01240, 2002.

758 Oksanen, J., Blanchet, F. G., Kindt, R., Legendre, P., and Minchin, P. R.: vegan: Community
759 ecology package. R package version 2.0-6. , 2013.

760 Oschlies, A., and Garcon, V.: Eddy-induced enhancement of primary production in a model of
761 the North Atlantic Ocean, Nature, 394, 266–269, 1998.

762 Pinheiro, J. C., Bates, D. M., DebRoy, S., Sarkar, D., and R Core Team: nlme: Linear and
763 nonlinear mixed effects models, R package version 3.1-120 ed., 2015.

764 Poretsky, R. S., Hewson, I., Sun, S. L., Allen, A. E., Zehr, J. P., and Moran, M. A.: Comparative
765 day/night metatranscriptomic analysis of microbial communities in the North Pacific subtropical
766 gyre, Environmental Microbiology, 11, 1358-1375, 10.1111/j.1462-2920.2008.01863.x, 2009.

767 Pruesse, E., Quast, C., Knittel, K., Fuchs, B. M., Ludwig, W., Peplies, J., and Glöckner, F. O.:
768 SILVA: a comprehensive online resource for quality checked and aligned ribosomal RNA
769 sequence data compatible with ARB, Nucleic acids research, 35, 7188–7196,
770 10.1093/nar/gkm864, 2007.

771 R Core Team: R: A language and environment for statistical computing, R Foundation for
772 Statistical Computing, Vienna, Austria, 2015.

773 Rappé, M. S., Connon, S. A., Vergin, K. L., and Giovannoni, S. J.: Cultivation of the ubiquitous
774 SAR11 marine bacterioplankton clade, Nature, 418, 630-633 doi:10.1038/nature00917, 2002.

775 Richardson, D. C., and Richardson, J. S.: The kinemage: A tool for scientific communication,
776 Protein Science, 1, 3-9, 10.1002/pro.5560010102, 1992.

777 Riebesell, U., and Gattuso, J.-P.: Lessons learned from ocean acidification research, Nature
778 Climate Change, 5, 2015.

779 Ryabenko, E., Kock, A., Bange, H. W., Altabet, M. A., and Wallace, D. W. R.: Contrasting
780 biogeochemistry of nitrogen in the Atlantic and Pacific oxygen minimum zones, Biogeosciences
781 9, 203-215, 2012.

782 Schloss, P. D., Westcott, S. L., Ryabin, T., Hall, J. R., Hartmann, M., and al., e.: Introducing
783 mothur: Open-source, platform-independent, community-supported software for describing and
784 comparing microbial communities, Applied and Environmental Microbiology, 75, 7537–7541, doi:
785 10.1128/aem.01541-09 2009.

786 Schmid, M. C., Hooper, A. B., Klotz, M. G., Woebken, D., Lam, P., Kuypers, M. M. M.,
787 Pommerening-Roeser, A., op den Camp, H. J. M., and Jetten, M. S. M.: Environmental detection
788 of octahaem cytochrome c hydroxylamine/hydrazine oxidoreductase genes of aerobic and
789 anaerobic ammonium-oxidizing bacteria, Environmental Microbiology, 10, 3140-3149,
790 10.1111/j.1462-2920.2008.01732.x, 2008.

791 Schütte, F., Karstensen, J., Krahmann, G., Fiedler, B., Brandt, P., Visbeck, M., and Körtzinger,
792 A.: Characterization of “dead-zone eddies” in the tropical North Atlantic Ocean, in prep for
793 Biogeosciences Discussion, 2015.

794 Stewart, F. J., Ulloa, O., and DeLong, E. F.: Microbial metatranscriptomics in a permanent
795 marine oxygen minimum zone, Environ Microbiol, 14, 23-40, 10.1111/j.1462-2920.2010.02400.x,
796 2011.

797 Stramma, L., Johnson, G. C., Sprintall, J., and Mohrholz, V.: Expanding oxygen-minimum zones
798 in the tropical oceans, Science, 320, 655-658, 10.1126/science.1153847, 2008.

799 Stramma, L., Bange, H. W., Czeschel, R., Lorenzo, A., and Frank, M.: On the role of mesoscale
800 eddies for the biological productivity and biogeochemistry in the eastern tropical Pacific Ocean
801 off Peru, Biogeosciences, 10, 7293-7306, doi:10.5194/bg-10-7293-2013, 2013.

802 Stratil, S. B., Neulinger, S. C., Knecht, H., Friedrichs, A. K., and Wahl, M.: Temperature-driven
803 shifts in the epibiotic bacterial community composition of the brown macroalga Fucus
804 vesiculosus. , MicrobiologyOpen, 10.1002/mbo1003.1079, 2013.

805 Stratil, S. B., Neulinger, S. C., Knecht, H., Friedrichs, A. K., and Wahl, M.: Salinity affects
806 compositional traits of epibacterial communities on the brown macroalga *Fucus vesiculosus*,
807 FEMS Microbiology Ecology, 88, 272–279, 10.1111/1574-6941.12292, 2014.

808 Suzuki, M., Preston, C., Chavez, F., and DeLong, E.: Quantitative mapping of bacterioplankton
809 populations in seawater: field tests across an upwelling plume in Monterey Bay, Aquatic
810 Microbial Ecology, 24, 117–127, 2001.

811 Swan, B. K., Martinez-Garcia, M., Preston, C. M., Sczyrba, A., Woyke, T., Lamy, D., Reinthaler,
812 T., Poulton, N. J., Masland, E. D. P., Gomez, M. L., Sieracki, M. E., DeLong, E. F., Herndl, G. J.,
813 and Stepanauskas, R.: Potential for chemolithoautotrophy among ubiquitous bacteria lineages in
814 the dark ocean, Science, 333, 1296–1300, 10.1126/science.1203690, 2011.

815 Ulloa, O., Canfield, D. E., DeLong, E. F., Letelier, R. M., and Stewart, F. J.: Microbial
816 oceanography of anoxic oxygen minimum zones, Proc. Natl. Acad. Sci. U. S. A., 109, 15996-
817 16003, 10.1073/pnas.1205009109, 2012.

818 Vaquer-Sunyer, R., and Duarte, C. M.: Thresholds of hypoxia for marine biodiversity, Proc. Natl.
819 Acad. Sci. USA. , 105, 15452–15457, 2008.

Wang, Q., Garrity, G. M., Tiedje, J. M., and Cole, J. R.: Naïve Bayesian Classifier for Rapid Assignment of rRNA Sequences into the New Bacterial Taxonomy, Appl. Environ. Microbiol. , 73, 5261-5267 doi: 10.1128/AEM.00062-07, 2007.

West, N. J., Lebaron, P., Strutton, P. G., and Suzuki, M. T.: A novel clade of Prochlorococcus found in high nutrient low chlorophyll waters in the South and Equatorial Pacific Ocean, ISME J, 5, 933-944, 2011.

Wright, J. J., Konwar, K. M., and Hallam, S. J.: Microbial ecology of expanding oxygen minimum zones, Nat. Rev. Microbiol., 10, 381-394, 10.1038/nrmicro2778, 2012.

Yu, Y., Lee, C., Kim, J., and Hwang, S.: Group-specific primer and probe sets to detect methanogenic communities using quantitative real-time polymerase chain reaction, 89, 670–679, 10.1002/bit.20347, 2005.

Zhu, M., and Ghodsi, A.: Automatic dimensionality selection from the scree plot via the use of profile likelihood, Computational Statistics & Data Analysis, 51, 918-930, 10.1016/j.csda.2005.09.010, 2006.

Zuur, A. F., Ieno, E. N., Walker, N. J., Saveliev, A. A., and Smith, G. M.: Mixed effects models and extensions in ecology with R, Statistics for Biology and Health, edited by: Gail, M., Krickeberg, K., Samet, J. M., Tsiatis, A., and Wong, W., Springer, 2009.

Figures

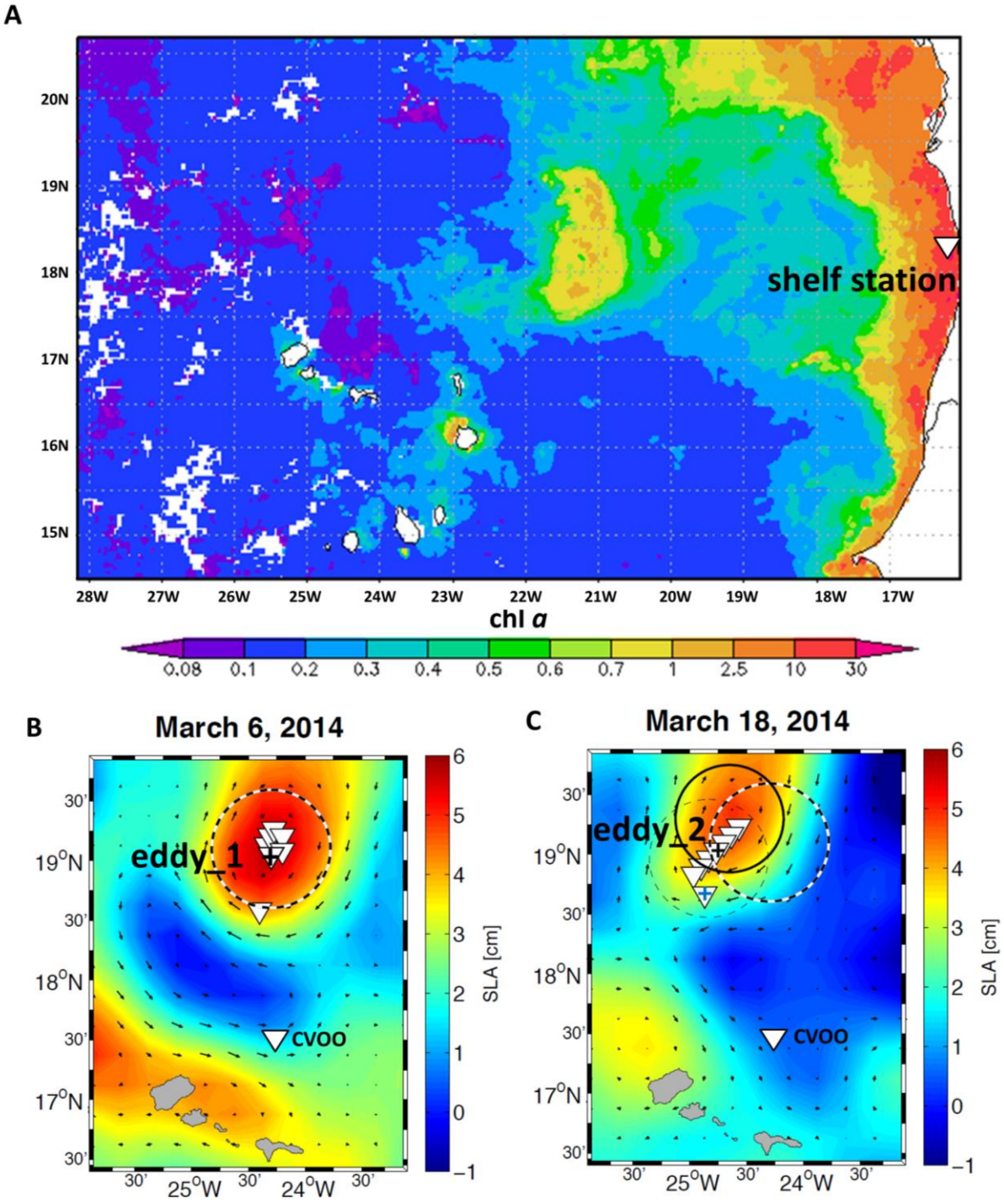

Figure 1: (A) MODIS-Aqua 4-km monthly mean chl*a* distribution in the ETNA (mg m^{-3}) in November 2013. Markedly increased chl*a* concentrations are associated with the low-oxygen ACME, located between 21°W and 22°W and 17.5°N and 19°N. Analyses and visualizations were produced with the Giovanni online data system, developed and maintained by the NASA GES DISC.

Eddy location indicated by sea level anomaly (SLA) during the time of the two surveys: (B) First eddy observation; + denotes the eddy_1 station, (C) Second eddy observation + denotes the eddy_2 station, an additional station was sampled at the eddy rim for C uptake measurements, indicated by the blue + White triangle marks the sampling station for the potential source water of the eddy. The dashed circles indicate the location of the eddy during the RV Islandia survey, the black circle indicates the eddy location during the RV Meteor survey, and the dashed black line indicates the direction of eddy propagation. Sampling stations are shown with white triangles.

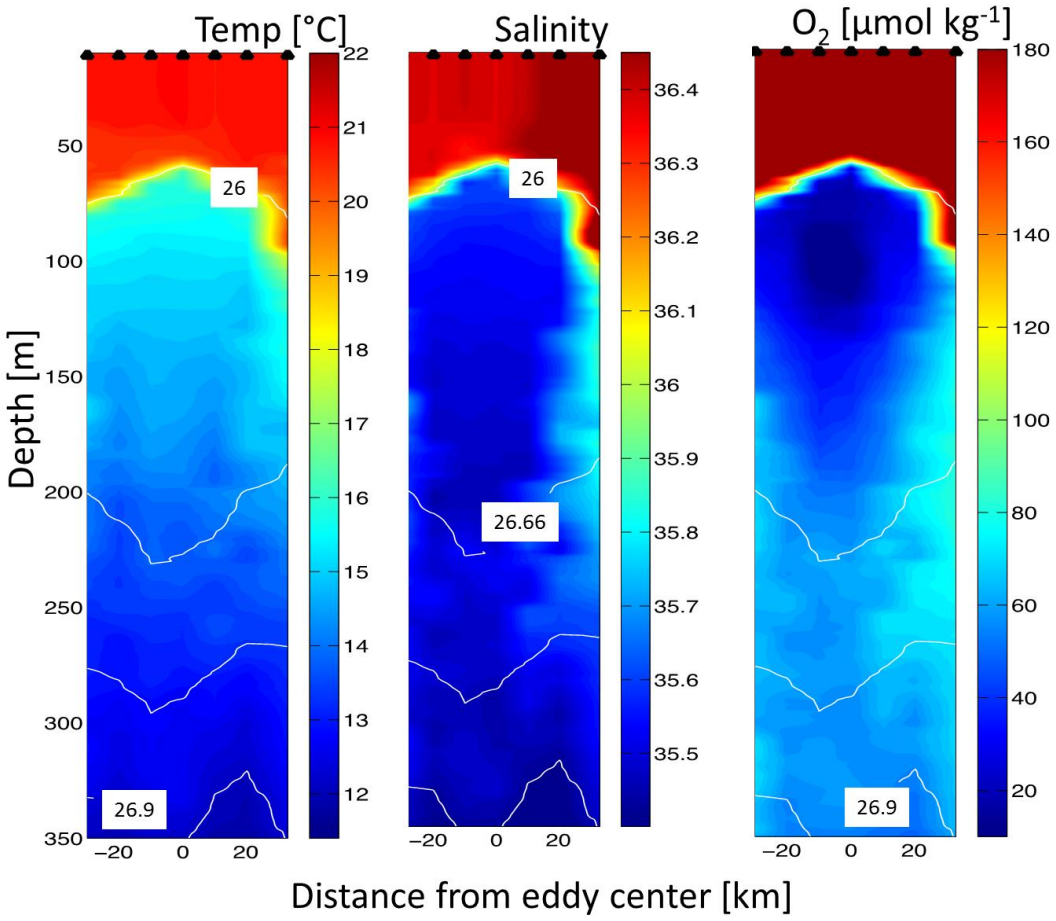

Figure 2: Temperature (left panel), salinity (middle panel) andO_2 concentration (right panel) measured during a section of RV Meteor Cruise M105 across the studied eddy. Minimum O_2 was 4.8 µmol kg^{-1} at ~100 m water depth on that section; however, even lower $O_2$was detected with a glider (1.2µmol kg^{-1}). Isopycnals are indicated by white lines.

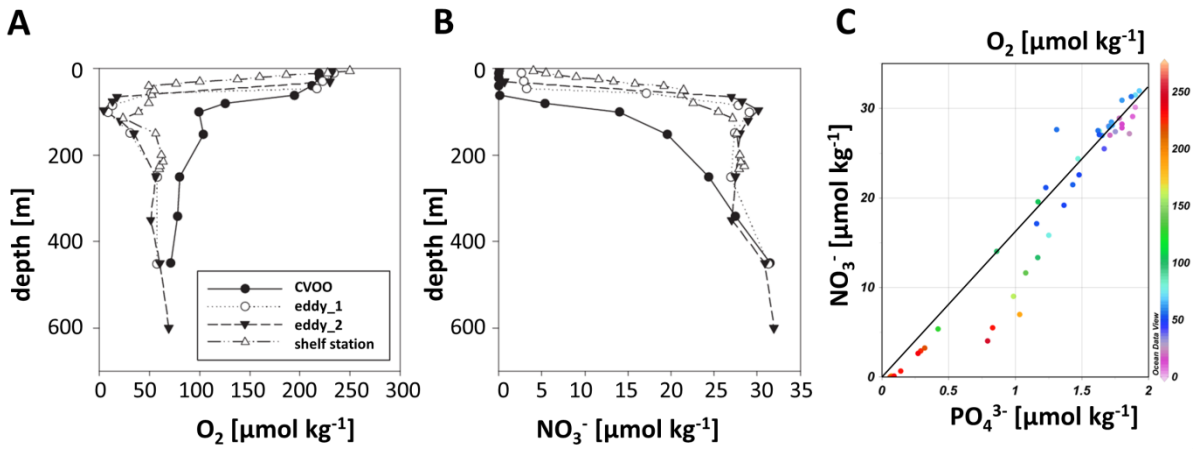

Figure 3: (A) O_2 and (B) nitrate (C) nitrite concentrations measured at the open ocean station CVOO (black circles), in the first observation (eddy_1, open circles), second observation (eddy_2, black triangles) and on the Mauritanian shelf (open triangles). (D) Nitrate vs. phosphate concentration at the 4 sampling stations. The color code denotes the O_2 concentration and the black line indicates the Redfield ratio of N:P = 16:1.

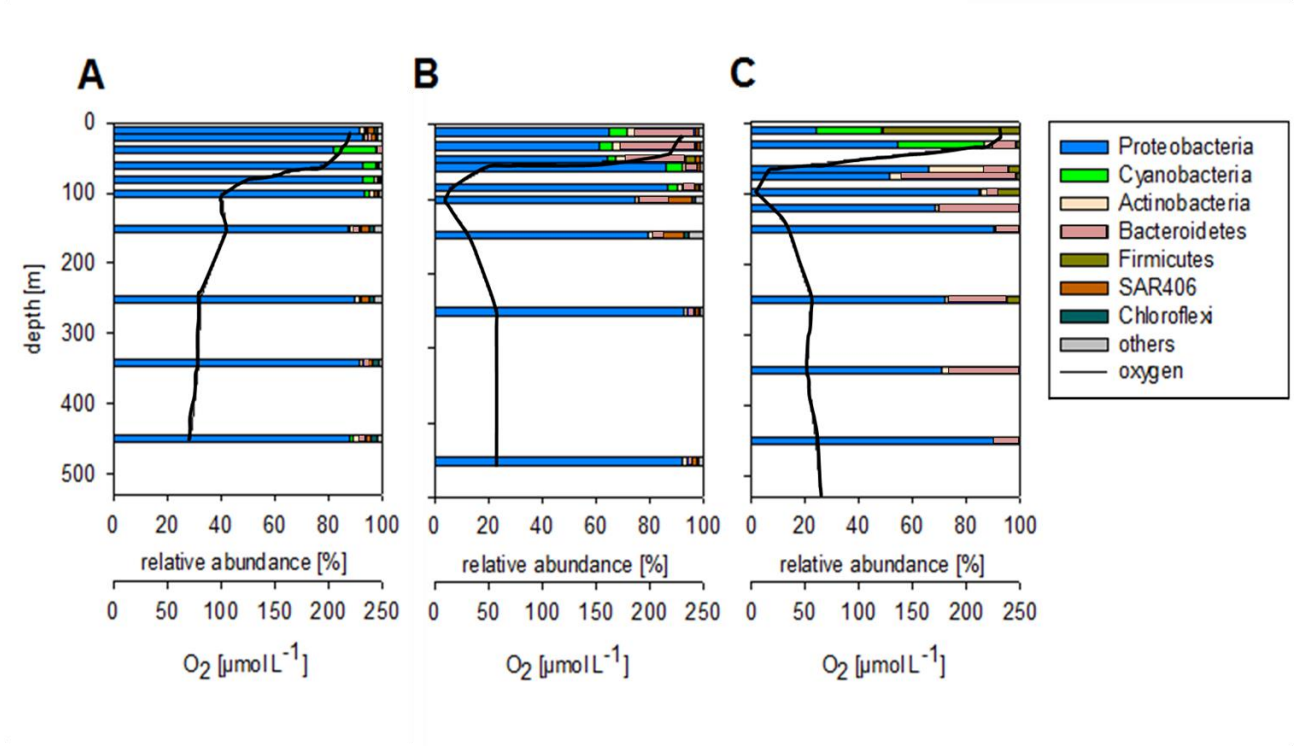

Figure 4: Distribution of bacterial phyla along vertical profiles of (A) CVOO, (B) first observation (eddy_1) and (C) second observation (eddy_2) is shown along with the O_2 gradient (black line). Datasets result from 16S rDNA amplicon sequencing (an overview on archaeal sequence distribution is given in the supplemental material).

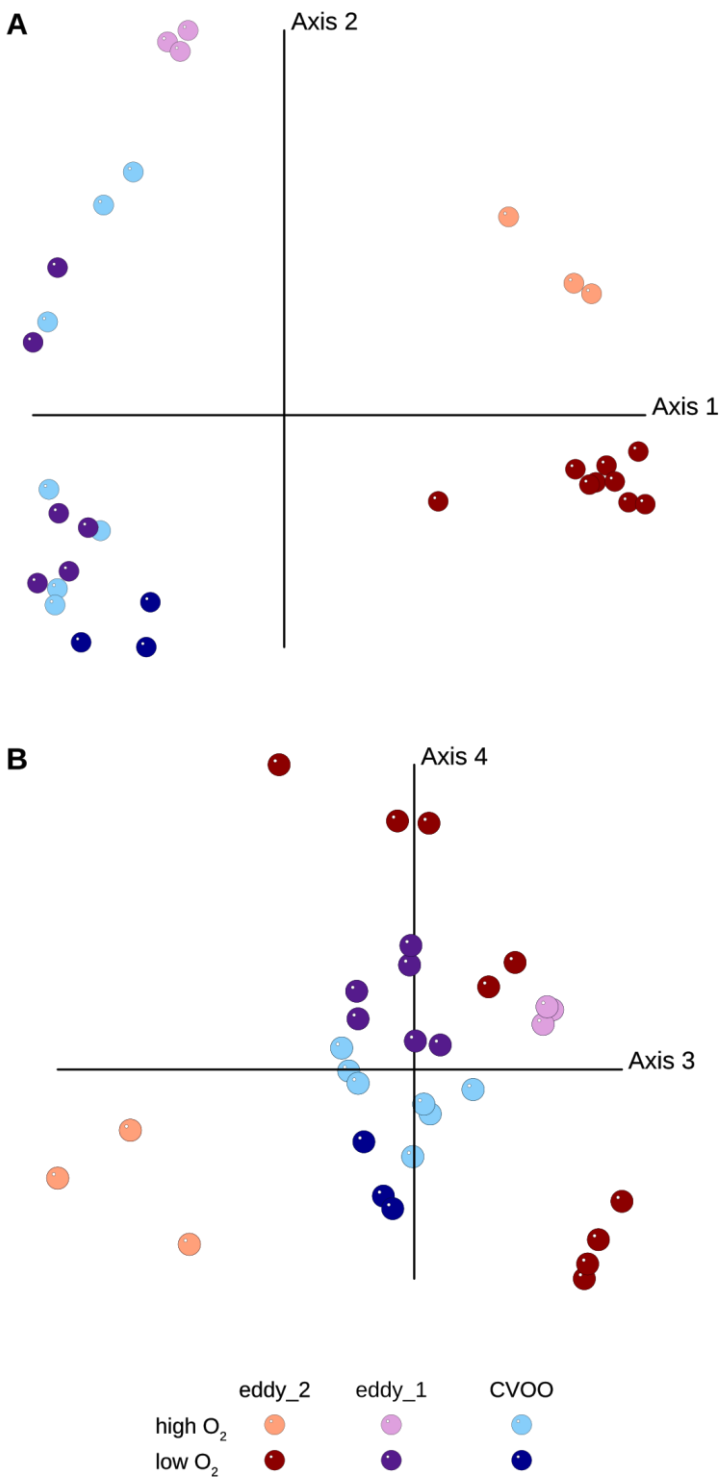

Figure 5: Redundancy analysis (RDA) of OTU distribution in samples from the first eddy observation (eddy_1), from the second eddy observation (eddy_2) and from CVOO based on 16S rDNA sequences. (A) First and second axis, (B) third and fourth axis of the RDA model, illustrating the interaction effect of factor "Realm" and O_2 concentration. For plotting, the continuous variable "O_2" was converted into a factor with two levels "high O_2" (>90 µM) and "low O_2" (≤90 µM).

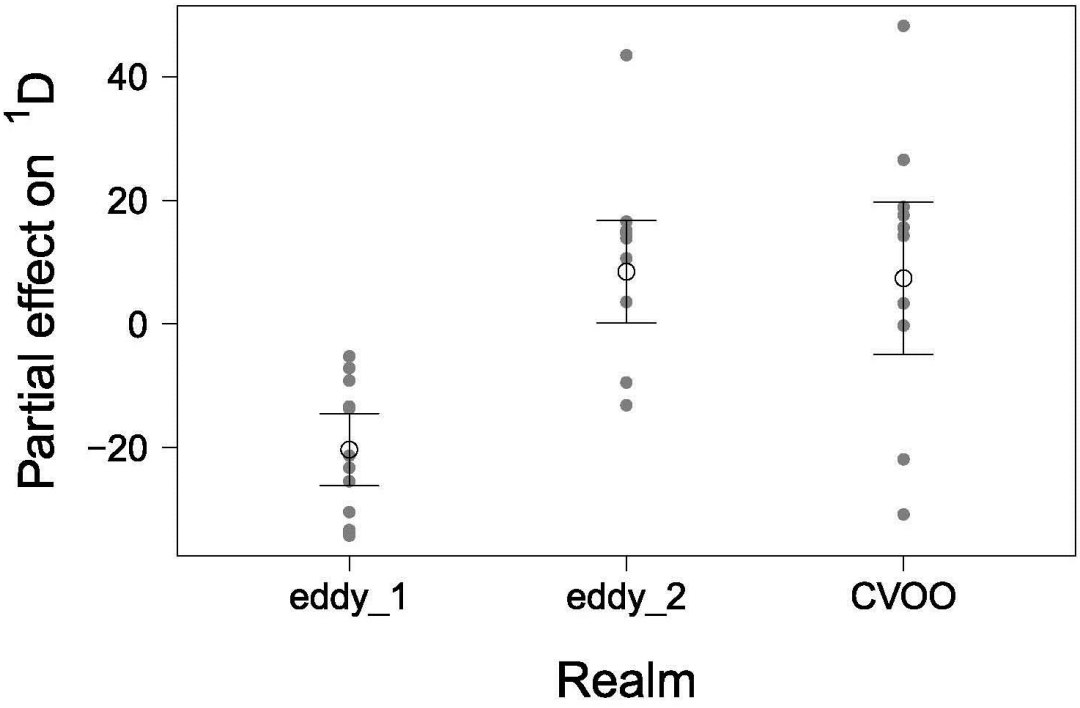

Figure 6: Alpha diversity analysis of eddy sampling stations (first observation (eddy_1), second observation (eddy_2)) and CVOO expressed as Shannon numbers equivalent (^1D). A strong and significant decrease in diversity is observed in the eddy. Partial response residuals (black symbols) were extracted from full GLS model re-fitted without the "Realm" main effect. Predicted values for partial residualsmodelled by the "Realm" main effect alone (and thus adjusted for differences in O_2 concentration) are shown as blue symbols. Error bars represent 95% confidence interval for fitted values.

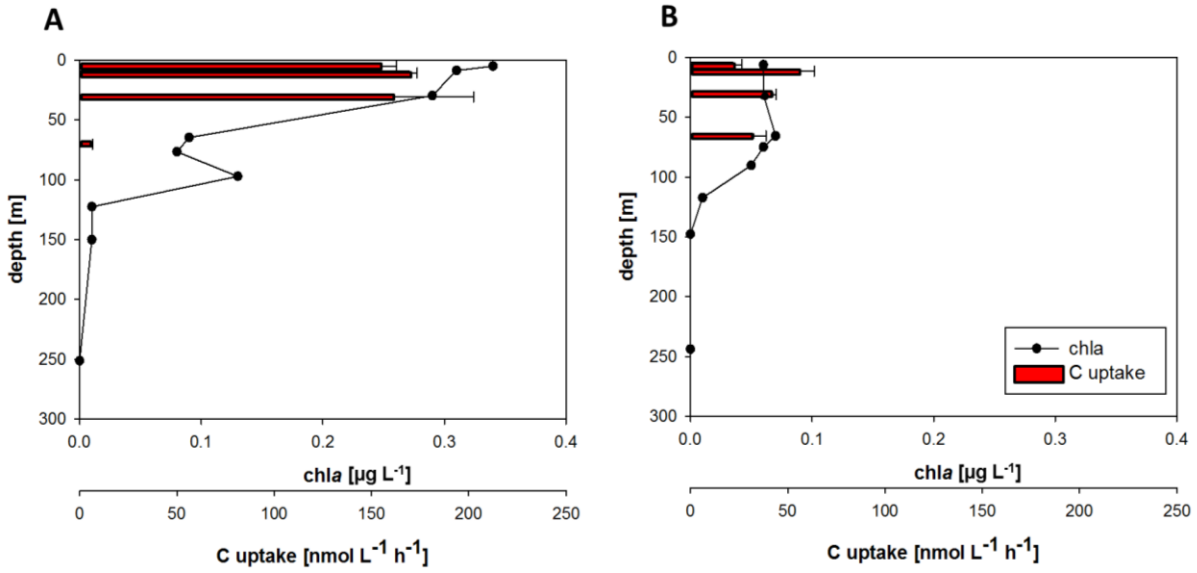

Figure 7: Chlorophyll *a* (chl*a*, µg L^{-1}) distribution as determined from discrete measurements and carbon uptake rates (A) inside the eddy (eddy_2, second observation) and (B) at the eddy rim (location denoted in Fig. 1). Error bars indicate the standard deviation of three replicate samples for C uptake.

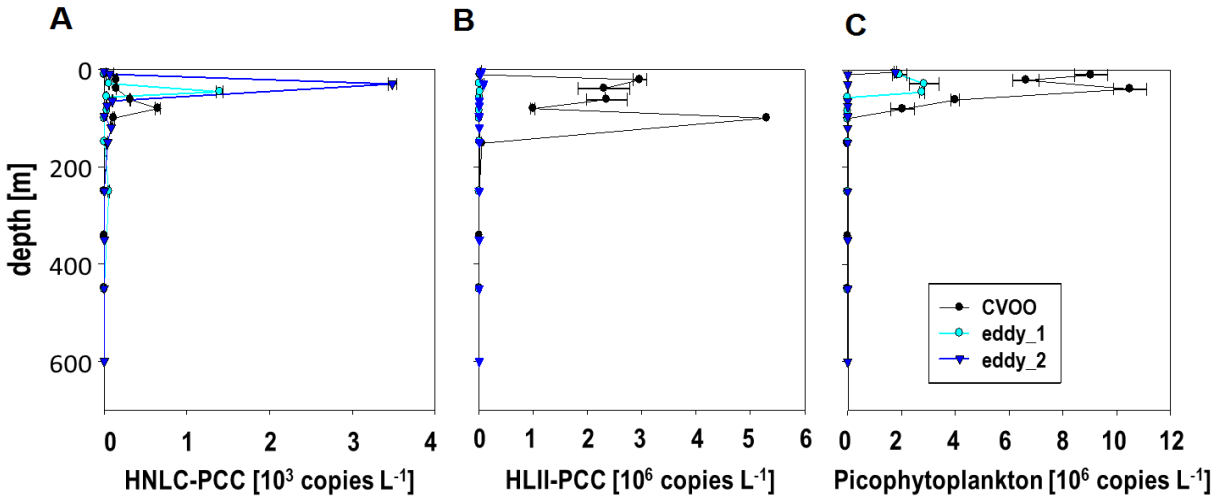

Figure 8: Vertical distribution of *Prochlorococcus* and *Synechococcus* ecotypes quantified by qPCR. While the HNLC-PCC (A) dominates the eddy water mass and increases from the first observation (eddy_1) to the second observation (eddy_2) it is nearly absent outside the eddy (CVOO). HLII-PCC (B) occurs in highest abundances outside the eddy, while being close to the detection limit inside the eddy. (C) shows the distribution of pico-phytoplankton as detected with a general primer-probe system (Suzuki et al., 2001).

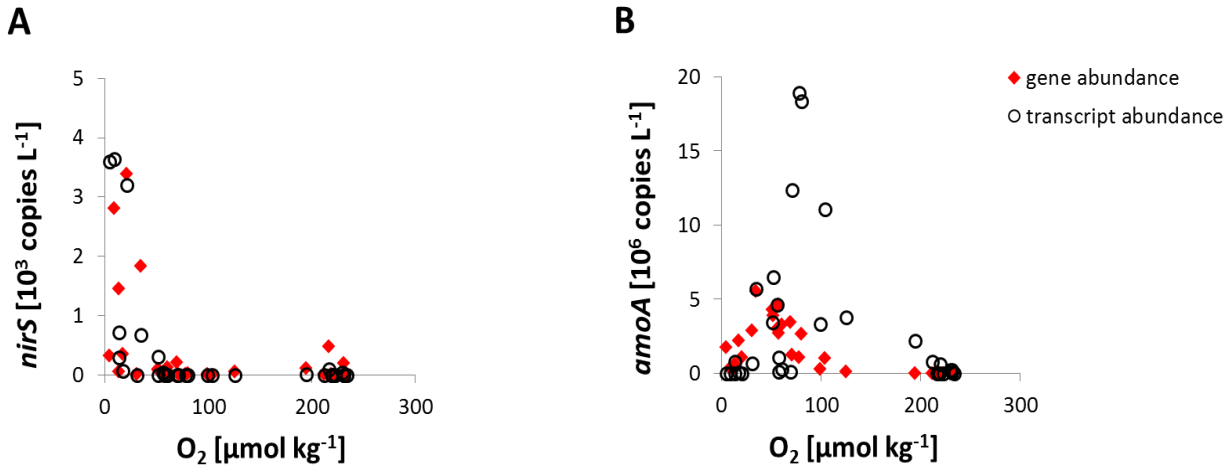

Figure 9: Gene and transcript abundance vs. O_2 concentrations of samples from the eddy observations (eddy_1 and eddy_2) and CVOO. (A) shows the key gene for denitrification, *nirS*, coding for the nitrite reductase, (B) shows archaeal *amoA* as key functional gene of ammonia oxidation, coding for the ammonia monooxygenase. Gene abundances are denoted in red, transcript abundances are indicated by black circles.